cells and regulatory T cells (Treg), as PL consisted of higher numbers of T cells (791.8 Helper T cells/mm2, 195.7 Treg/mm2) than LM (626.3 Helper T cells/mm2, 121.3 Treg/mm2). However, cytotoxic T cells exhibiting GZB+ and CTLA-4- were fewer in PL (140.2 cells/mm2) than in LM (203.3 cells/mm2), and the ratio is 0.69. The mean number of GZB+ TIL in PL (32.5 cells/mm2) was lower than in LM (35.3 cells/mm2), and their proportions among total TIL counts were 0.12 and 0.31, respectively. In PL, GZB+: GZB- ratio is 0.16 while the ratio is 1.91 for LM. A fewer number of TILs exhibiting GZB suggests that PL has lower efficiency in immune response than LM. Another crucial checkpoint receptor that inhibits immune response, CTLA-4, was more prevalent in PL, with CTLA-4+: CTLA-4- ratio in Treg being 0.36 in PL, compared to 0.11 in LM. The tumor proportion score (TPS) of PD-L1 was higher in PL than LM (40.0 vs. 6.6).

Conclusions In our study, we showed the differences in the numbers of TIL or regulatory T cells and expressions of immune checkpoint receptors (PD-L1, CTLA-4), which significantly influence outcomes for CIT. The study is ongoing to confirm different IME between the PL and LM groups in a larger tumor cohort.

REFERENCES

1. Peng, Jianhong, *et al*., Immune Cell Infiltration in the Microenvironment of Liver Oligometastasis from Colorectal Cancer: Intratumoural CD8/CD3 Ratio Is a Valuable Prognostic Index for Patients Undergoing Liver Metastasectomy. *Cancers* 2019 Dec; **11**(12): 1922. https://doi.org/10.3390/cancers11121922
2. Tumeh, Paul C., *et al*., Liver Metastasis and treatment outcome with Anti-PD-1 monoclonal antibody in patients with melanoma and NSCLC. *Cancer Immunol Res* 2017 May; **5**(5): 417–424. doi: 10.1158/2326-6066.CIR-16-0325
3. Parra, E.R., Immune Cell Profiling in Cancer Using Multiplex Immunofluorescence and Digital Analysis Approaches; Streckfus, C.F., Ed.; IntechOpen: London, UK, 2018; pp. 1–13. doi: 10.5772/intechopen.80380
4. Ribas, A., Hu-Lieskovan, S., What does PD-L1 positive or negative mean?. *The Journal of Experimental Medicine* 2016;213(13):2835–2840. https://doi.org/10.1084/jem.20161462

http://dx.doi.org/10.1136/jitc-2020-SITC2020.0747

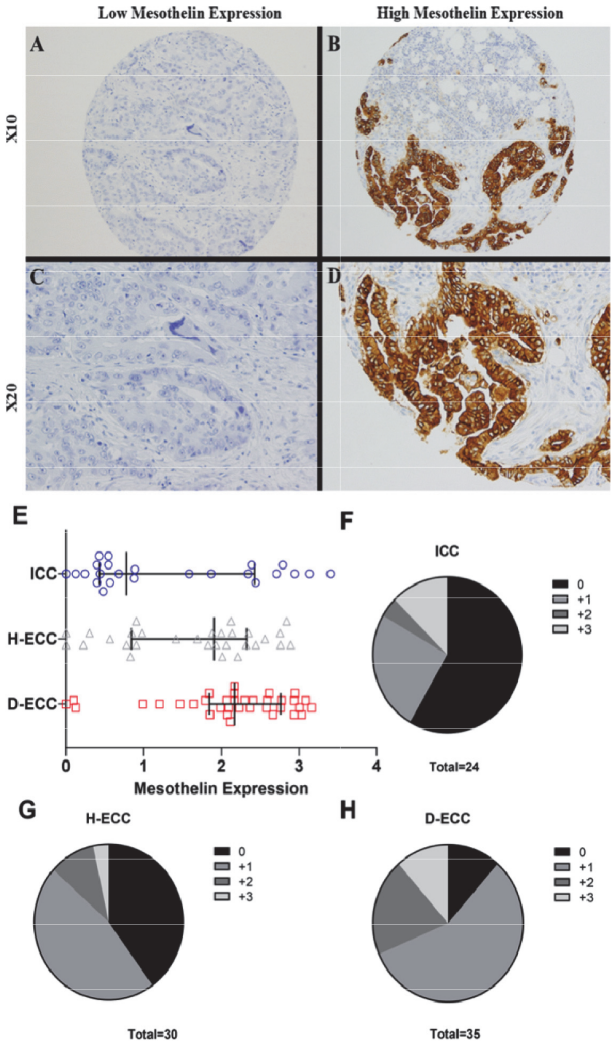

Abstract 748 Figure 1 Mesothelin expression by primary tumor location
A+C) Representative low Mesothelin expression at low (X10) (A) and higher power (X20) (C). B+D) Representative high Mesothelin expression at low (X10)(B) and higher power (X20)(D). E) Log(x+1) transformed Mesothelin Expression as determined by automated cell counting, median and IQR, all data points shown. Median: 5.5, 79.5, 146.0 for ICC, H-ECC, D-ECC, respective, p-value = 0.025. F-H) Mesothelin Expression determined by visual inspection and scoring for ICC (F), H-ICC (G), and D-ECC (D).

748 MYELOID CELL INFILTRATION CORRELATES WITH PROGNOSIS AND VARIES BASED ON TUMOR LOCATION IN CHOLANGIOCARCINOMA

Paul Kunk, Sean Dougherty*. *University of Virginia, Charlottesville, VA, USA*

Background Cholangiocarcinoma (CC) is a rare malignancy with an increasing incidence and poor prognosis. Immunotherapy represents one potential treatment for CC, however identification of immunotherapeutic targets requires a thorough characterization of the tumor immune microenvironment (TIME). Mesothelin, a tumor associated antigen, is abundantly expressed in other malignancies, though its expression in CC has not been well characterized. We hypothesized that (1) the TIME of CC would vary by primary tumor location and between primary and metastatic lesions, (2) high tumor infiltration by CD8+ T cells and low infiltration by M2 macrophages would be associated with improved survival, and (3) most CC would express mesothelin.

Methods 99 CC tumors from unique stage I-IV patients were included, of which 89 were primary tumors (24 intrahepatic (ICC), 65 extrahepatic (ECC - 30 hilar (H-ECC) and 35 distal (D-ECC))) and 10 were metastatic lesions. Tissue microarrays were constructed and immunohistochemistry (IHC) was performed for lymphoid and myeloid markers, as well as for PD-L1 and mesothelin. IHC+ cells were quantified by automated image analysis. Expression of mesothelin and PD-L1 by tumors cells were evaluated on a semiquantitative scale (0, +1, +2, or +3). Hypothesis testing was performed using Kruskal-Wallis test and survival analyses were performed with Univariate and Multivariate Cox Hazard Models.

Results Most tumors were infiltrated by myeloid cells in addition to CD4+, CD8+, and FoxP3+ T-cells. Mesothelin was expressed (≥1+) in 68% of tumors (figure 1), while PD-L1 was expressed (≥1%) in only 16% of tumors. Higher densities of M1 macrophages (CD68+) were present in D-ECC relative to ICC and H-ECC (figure 2). M1 macropahges were also found in higher densities in metastatic tumors. Mesothelin and granzyme-B expression was significantly higher in D-ECC. Increasing density of myeloid cells (CD14+) and M2 macrophages (CD163+) was associated with worse survival (p= 0.02, 0.03, respectively) (figure 3). Intraepithelial and intratumoral T cell infiltration did not correlate with OS.

J Immunother Cancer: first published as 10.1136/jitc-2020-SITC2020.0748 on 9 November 2020. Downloaded from http://jitc.bmj.com/ on April 29, 2024 by guest. Protected by copyright.

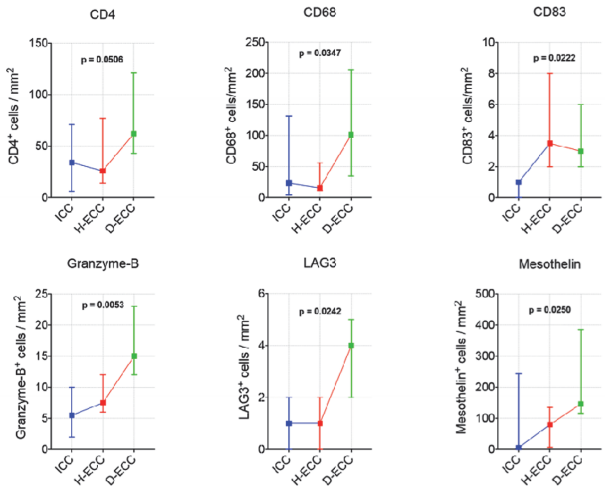

Abstract 748 Figure 2 Immune infiltration based on primary tumor location
Increase in immune infiltrate in primary tumors as distance from liver increases. P-values determined by Jonckheere-Terpstra Test with FDR corrections

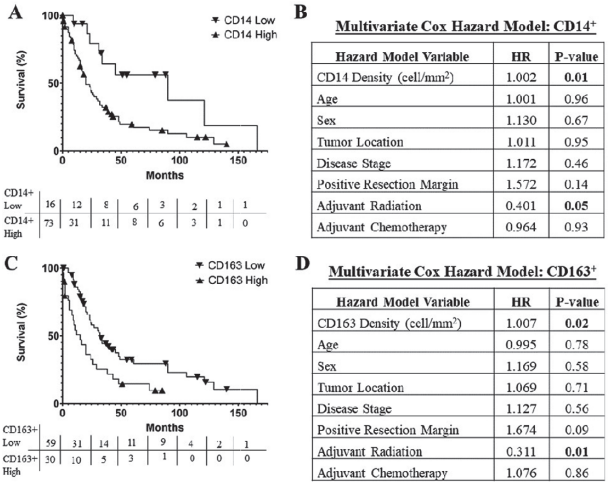

B **Multivariate Cox Hazard Model: CD14+**

Hazard Model Variable	HR	P-value
CD14 Density (cell/mm²)	1.002	**0.01**
Age	1.001	0.96
Sex	1.130	0.67
Tumor Location	1.011	0.95
Disease Stage	1.172	0.46
Positive Resection Margin	1.572	0.14
Adjuvant Radiation	0.401	**0.05**
Adjuvant Chemotherapy	0.964	0.93

D **Multivariate Cox Hazard Model: CD163+**

Hazard Model Variable	HR	P-value
CD163 Density (cell/mm²)	1.007	**0.02**
Age	0.995	0.78
Sex	1.169	0.58
Tumor Location	1.069	0.71
Disease Stage	1.127	0.56
Positive Resection Margin	1.674	0.09
Adjuvant Radiation	0.311	**0.01**
Adjuvant Chemotherapy	1.076	0.86

Abstract 748 Figure 3 CD14 and CD163 Correlate with OS
A+C) Kaplan Meier Curve of OS for (A) CD14 (Median OS: 20 vs. 90 months, log-rank p-value <0.01) and (C) CD163 (Median OS: 15 vs. 32 months, log-rank p-value<0.01). B+D) Multivariate Cox Hazard Models. Assumptions of Cox Hazard Model were checked with Schoenfeld residual values, significance level <0.01

Conclusions The TIME of CC varies significantly by primary tumor location and between primary and metastatic lesions. D-ECC has a favorable immune profile compared to ICC and H-ECC, with a better milieu for antigen presentation including increased mesothelin and less suppressive macrophages, which may support better response to checkpoint blockade. The data supported the hypothesis that higher densities of intra-tumoral M2 macrophages and myeloid cells correlated with worse OS, even after controlling for clinical variables, suggesting that these cell populations may represent promising immunotherapeutic targets in CC.

http://dx.doi.org/10.1136/jitc-2020-SITC2020.0748

749 SPATIAL PROFILING OF THE TUMOUR MICROENVIRONMENT IN HEAD AND NECK CANCER TO IDENTIFY BIOMARKERS OF RESPONSE TO THERAPY

Arutha Kulasinghe*. *Queensland University of Technology, Kelvin Grove, Australia*

Background Immune checkpoint inhibitors (ICI) have shown durable and long-term benefits in a subset of head and neck squamous cell carcinoma (HNSCC) patients. To identify patient-responders from non-responders, biomarkers are needed which are predictive of outcome to ICI therapy. Cues in the tumour microenvironment (TME) have been informative in understanding the tumour-immune contexture.
Methods In this study, the NanoString GemoMx™ Digital Spatial Profiling (DSP) technology was used to determine the immune marker and compartment specific measurements in a cohort of HNSCC tumours from patients receiving ICI therapy.
Results Our data revealed that markers involved with immune cell infiltration (CD8 T-cells) were not predictive of outcome to ICI therapy. Rather, a number of immune cell types (CD4, CD68, CD45, CD44, CD66b) were found to correlate with progressive disease.
Conclusions This study, to our knowledge, represents the first spatial analysis of HNSCC tumours.
Ethics Approval The study was approved by the Queensland University of Technology Ethics Board.

http://dx.doi.org/10.1136/jitc-2020-SITC2020.0749

750 MALAT1 LNCRNA CONTROLS METASTATIC REACTIVATION OF DORMANT BREAST CANCER BY IMMUNE EVASION

Dhiraj Kumar*, Sreeharsha Gurrapu, Hyunho Han, Yan Wang, Seongyeon Bae, Hong Chen, Chang-Jiun Wu, Filippo Giancotti. *The University of Texas MD Anderson Cancer Center, Houston, TX, USA*

Background Long non-coding RNAs (lncRNAs) are involved in various biological processes and diseases. Malat1 (metastasis-associated lung adenocarcinoma transcript 1), also known as Neat2, is one of the most abundant and highly conserved nuclear lncRNAs. Several studies have shown that the expression of lncRNA Malat1 is associated with metastasis and serving as a predictive marker for various tumor progression. Metastatic relapse often develops years after primary tumor removal as a result of disseminated tumor cells undergoing a period of latency in the target organ.[1–4] However, the correlation of tumor intrinsic lncRNA in regulation of tumor dormancy and immune evasion is largely unknown.
Methods Using an in vivo screening platform for the isolation of genetic entities involved in either dormancy or reactivation of breast cancer tumor cells, we have identified Malat1 as a positive mediator of metastatic reactivation. To functionally uncover the role of Malat1 in metastatic reactivation, we have developed a knock out (KO) model by using paired gRNA CRISPR-Cas9 deletion approach in metastatic breast and other cancer types, including lung, colon and melanoma. As proof of concept we also used inducible knockdown system under in vivo models. To delineate the immune microenvironment, we have used 10X genomics single cell RNA-seq, ChIRP-seq, multi-color flowcytometry, RNA-FISH and immunofluorescence.
Results Our results reveal that the deletion of Malat1 abrogates the tumorigenic and metastatic potential of these tumors

J Immunother Cancer: first published as 10.1136/jitc-2020-SITC2020.0748 on 9 November 2020. Downloaded from http://jitc.bmj.com/ on April 29, 2024 by guest. Protected by copyright.